CHANGES IN TROPICAL RAINFALL MEASURING MISSION (TRMM) RETRIEVALS DUE TO THE ORBIT BOOST ESTIMATED FROM RAIN GAUGE DATA

A Thesis

by

JEREMY DEMOSS

Submitted to the Office of Graduate Studies of
Texas A&M University
in partial fulfillment of the requirements for the degree of

MASTER OF SCIENCE

August 2006

Major Subject: Atmospheric Sciences

CHANGES IN TROPICAL RAINFALL MEASURING MISSION (TRMM) RETRIEVALS DUE TO THE ORBIT BOOST ESTIMATED FROM RAIN GAUGE DATA

A Thesis

by

JEREMY DEMOSS

Submitted to the Office of Graduate Studies of
Texas A&M University
in partial fulfillment of the requirements for the degree of

MASTER OF SCIENCE

Approved by:

Co-Chairs of Committee,	Kenneth P. Bowman
	Gerald R. North
Committee Members,	Benjamin Giese
Head of Department,	Richard E. Orville

August 2006

Major Subject: Atmospheric Sciences

ABSTRACT

Changes in Tropical Rainfall Measuring Mission (TRMM) Retrievals Due to the Orbit Boost Estimated from Rain Gauge Data. (August 2006)

Jeremy DeMoss, B.S., Union University

Co–Chairs of Advisory Committee: Dr. Kenneth P. Bowman
Dr. Gerald R. North

During the first three-and-a-half years of the Tropical Rainfall Measuring Mission (TRMM), the TRMM satellite operated at a nominal altitude of 350 km. To reduce drag, save maneuvering fuel, and prolong the mission lifetime, the orbit was boosted to 403 km in August 2001. The change in orbit altitude produced small changes in a wide range of observing parameters, including field-of-view size and viewing angles. Due to natural climatic variability, it is not possible to evaluate possible changes in precipitation retrievals from the satellite data alone. We estimate changes in TRMM Microwave Imager (TMI) and the Precipitation Radar (PR) precipitation retrievals due to the orbit boost by comparing them with surface rain gauges on ocean buoys operated by the NOAA Pacific Marine Environment Laboratory (PMEL). For each rain gauge, we compute the bias between the satellite and the gauge for pre- and post-boost time periods. For the TMI, the satellite is biased $\sim$12% low relative to the gauges during the pre-boost period and $\sim$1.5% low during the post-boost period. The mean change in bias relative to the gauges is approximately 0.4 mm day^{-1}. The PR is biased significantly low relative to the gauges during both boost periods. The change in bias is rain rate dependent, with larger changes in areas with higher mean precipitation rates.

To my friends and family.

ACKNOWLEDGMENTS

I want to thank Dr. K.P. Bowman and Dr. G.R. North for providing me the opportunity to be a part of the Department of Atmospheric Sciences graduate program. I would like to thank Dr. Bowman for guiding and helping me with any problems I had as I conducted this research. I am grateful to Dr. Benjamin Giese for serving on my thesis committee. In addition, I would like to thank the Texas A&M Atmospheric Sciences faculty for providing me graduate level education over the past two years.

Funding was provided by NASA Global Precipitation Mission Grant NAG5-4753 to Texas A&M University. I would like to thank TSDIS and the TRMM algorithm development teams for processing and archiving the TRMM data. Thanks also to Mike McPhaden, Yoande Serra, and NOAA/PMEL for providing access to the ocean buoy data.

Salil Mahajan, Qiaoyan Wu, and Dr. Tatiana Erukhimova have helped me greatly with IDL programming and various other things, and I thank them.

TABLE OF CONTENTS

LIST OF TABLES

LIST OF FIGURES

FIGURE Page

CHAPTER I

INTRODUCTION

The Tropical Rainfall Measuring Mission (TRMM) satellite, a joint U.S.-Japan mission, was launched in November 1997. TRMM provides data from 40°N to 40°S, covering the tropics and subtropics. TRMM is equipped with two primary instruments for measuring rainfall: the TMI (TRMM Microwave Imager) and the PR (Precipitation Radar). The TMI is a conically-scanning microwave radiometer that operates at five different frequencies and provides information on several precipitation variables. Over the ocean the TMI infers precipitation primarily based on microwave radiation emission from raindrops; that is, rain appears warm against the cold ocean below. Over land, TMI retrievals depend principally on ice scattering of short wavelength radiation in deep clouds. As a result, the TMI retrievals are more directly related to surface rain over the ocean. The PR is an electronically scanning radar that measures backscattered radiation. It infers surface rainfall rates from the reflectivity profile near the surface. The TRMM instruments are described in more detail in Kummerow et al. (1998).

TRMM was originally launched into a low (350 km altitude) orbit to maximize the sensitivity and ground resolution of the instruments. The orbit was boosted from 350 to 403 km in August 2001 to reduce drag and save maneuvering fuel, thereby prolonging the mission lifetime. The boost increased the swath width and field-of-view size for all of the instruments on the satellite. For the TMI, the swath width increased from 760 to 878 km, and the field-of-view from 4.4 to 5.1 km (at the highest resolution of 85.5 GHz). For the PR, the swath width increased from 215 to 247 km,

---

The journal model is *Journal of Climate*.

and the nadir field-of-view from 4.3 to 5.0 km. In addition to an increase in the area of measurements, the change in the viewing angle at the Earth's surface affected certain other parameters, such as the emissivity of the ocean surface. As a result, the orbit boost potentially affected the measurements in a variety of ways.

The goal of this study is to estimate the effects of the orbit boost on the TRMM rain rate retrievals. Because changes in precipitation retrievals due to the orbit boost cannot be distinguished easily from real climatic variations, we compare the TRMM retrievals to surface measurements of rainfall by rain gauges on ocean buoys, which are not affected by the orbit boost. The difficulty of this comparison is overcoming the sampling limitations of the two observing systems.

In addition to analyzing the orbit boost, we compare the TMI and PR instruments with each other. Previous work with the Version 5 TRMM data has shown that the bias between the TMI and gauges was near zero, while the PR was biased low with respect to the gauges (Bowman et al. 2003). Previous studies have also shown that the TMI typically measures more rainfall than the PR (Kummerow et al. 2000; Masunaga et al. 2002; Bowman et al. 2003; Serra and McPhaden 2003; Nesbitt et al. 2004; Furuzawa and Nakamura 2005; Bowman et al. 2005). The retrieval algorithms were updated in March 2004 and data were reprocessed. Version 6 data products are used in this study.

CHAPTER II

DATA AND METHODS

A. Data

For ground-truth, we use data from the NOAA TAO/TRITON/PIRATA ocean buoy array. The Tropical Atmosphere-Ocean (TAO) Project began in the mid-1980s in an attempt to gain a better understanding of El Niño events. The Tropical Atmosphere-Ocean Array/Triangle Trans-Ocean Buoy Network (TAO/TRITON) consists of 70 moorings in the tropical Pacific, and was completed in December 1994. Since that time, buoy data are available throughout the tropical Pacific, although not all buoys carry rain gauges. For tropical Atlantic locations, buoys from the Pilot Research Moored Array in the Tropical Atlantic (PIRATA) are used for analysis. The TAO/TRITON/PIRATA buoys are operated by the National Oceanic and Atmospheric Administration/Pacific Marine Environmental Laboratory (NOAA/PMEL). Details of the rain gauge measurements can be found in Hayes et al. (1991); McPhaden et al. (1998); Serra et al. (2001); and Serra and McPhaden (2003).

In this project, rain gauges on buoys throughout the tropical Atlantic and Pacific Oceans are used for comparison with the satellite data. An advantage of these rain gauges over gauges on islands is that they are not affected by local orographic and land surface-heating effects, so they should be representative of open-ocean rain rates.

Thirty-six rain gauges with at least 8 months of data in both the pre- and post-boost periods are used in this study; buoys with shorter data records are excluded. The buoys are numbered arbitrarily and are referenced by these numbers later in this paper (Figure 1). The rain gauges are R.M. Young capacitance-type gauges that measure the volume collected in the gauge at one-minute intervals. A Hanning filter

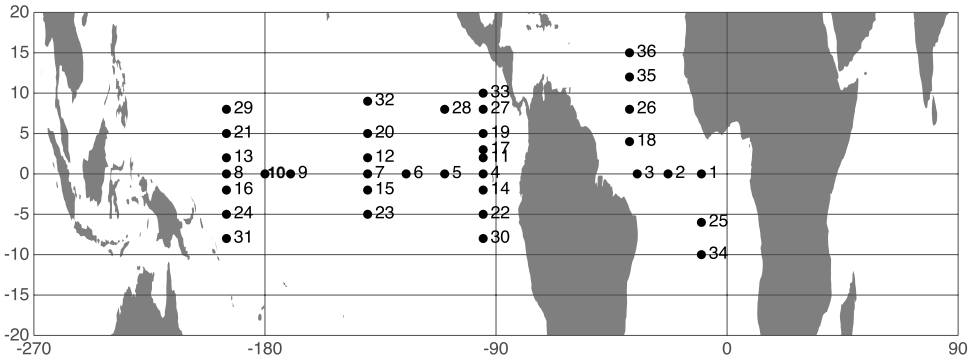

Fig. 1. Map of buoy locations. The buoys are numbered arbitrarily and are referenced throughout the paper with these numbers.

is used to smooth the noise in the volume measurements and produce filtered rain rates at 10-minute intervals (Serra et al. 2001).

1. TRMM Data

Version 6 of the TRMM 3G68 data are used here. TRMM 3G68 data products are rain-rate retrievals area averaged over 0.5°× 0.5° longitude-latitude grid boxes, resulting in 720 longitude grid boxes and 160 latitude grid boxes (40°S to 40°N). The satellite has a low-inclination orbit (35°) that precesses with respect to the diurnal cycle with a period of approximately 47 days.

The TRMM 3G68 product includes TMI, PR, and combined retrievals. We use only the TMI and PR products for comparison with rain gauges in this study. Results from the combined retrievals are very similar to the TMI. For some parts of the analysis we use the monthly-mean TMI retrievals on a $0.5^\circ \times 0.5^\circ$ grid (3A12 data product).

Data are available for TMI and PR from the launch of the TRMM satellite in December 1997 to the present (in this study, October 2005). For this study, the TRMM data are averaged over $1^\circ \times 1^\circ$ boxes to assure that the buoys lie near the center of the grid boxes, as the buoy positions wander slightly. During the eight-year period analyzed in this study (2557 days), approximately 3,600 TMI and 1,420 PR overpasses are available for a typical $1^\circ \times 1^\circ$ grid box.

B. Methods

1. Matching

One difficulty in comparing TRMM and gauge data lies in the fact that gauges have high temporal resolution at a point, while TRMM data have low temporal resolution and broad spatial coverage. This is due to the fact that the satellite views a given location approximately once per day, while rain gauges have nearly continuous measurements. To provide the best possible comparisons, the buoy data are matched with TRMM overpasses.

The gauge data are time averaged in a 6-hour window centered on each TRMM overpass. This time averaging provides near optimal comparison of the two observing systems (Bowman 2005). At some locations, there are substantial gaps in the gauge data; thus, there are usually many fewer matches at each buoy location than the actual number of TRMM overpasses.

2. Orbit Boost

In August 2001 the TRMM satellite orbit was boosted from 350 km to 403 km nominal altitude. To evaluate the effects of the boost, the measurements from the buoys and satellite are separated into pre- and post-boost categories. The period August 7, 2001 to August 24, 2001 is omitted from the analysis. Biases are computed relative to the gauges. The pre-boost bias between the satellite and a single gauge is defined as

$$\Delta r_{pre} = \langle r_{TRMM} \rangle_{pre} - \langle r_{buoy} \rangle_{pre}, \tag{2.1}$$

where angle brackets indicate the average over all matches and the subscripts indicate the data source and time period. Similarly, the post-boost bias is

$$\Delta r_{post} = \langle r_{TRMM} \rangle_{post} - \langle r_{buoy} \rangle_{post}. \tag{2.2}$$

Finally, we subtract the pre-boost bias from the post-boost bias to give the overall change in bias due to the orbit boost:

$$\Delta r = \Delta r_{post} - \Delta r_{pre}. \tag{2.3}$$

CHAPTER III

RESULTS

A. Data availability

Figure 2 shows the record of data availability for each rain gauge over the study period. The solid black bars represent the periods where gauge data are available at each buoy location. The single vertical lines represent the start and end of the TRMM data and the double lines represent the start and end of the boost period.

TMI and PR data are available consistently throughout this time period, with only a few missing days. At the launch of the TRMM satellite in December 1997, only a few of the rain gauges were operating, but more gauges became available shortly after. Thus, most of the gauges did not observe the strong 1997-1998 El Niño. Since TRMM data are almost continuous over the entire time period, the number of matches for each buoy location is primarily controlled by the gauge data availability.

B. Comparing single TRMM overpasses with gauge data

At each buoy the TRMM overpasses are matched with the 6-hour time-mean gauge value, centered on the satellite overpasses. To illustrate, we show scatterplots and histograms of TMI and PR versus gauge data for the full mission for selected buoys in different precipitation regimes.

Buoy 21 is located at a climatologically wet location that lies in the inter-tropical convergence zone (ITCZ) in the western Pacific (Figure 3). The number of TMI matches for this particular location is 2,652, of which 1,362 are raining in the TMI retrievals. The gauge mean for buoy 21 is 8.76 mm day^{-1}, while the TMI mean is 8.15 mm day^{-1}. There are 1,042 matches PR-gauge matches for this buoy, of which 665

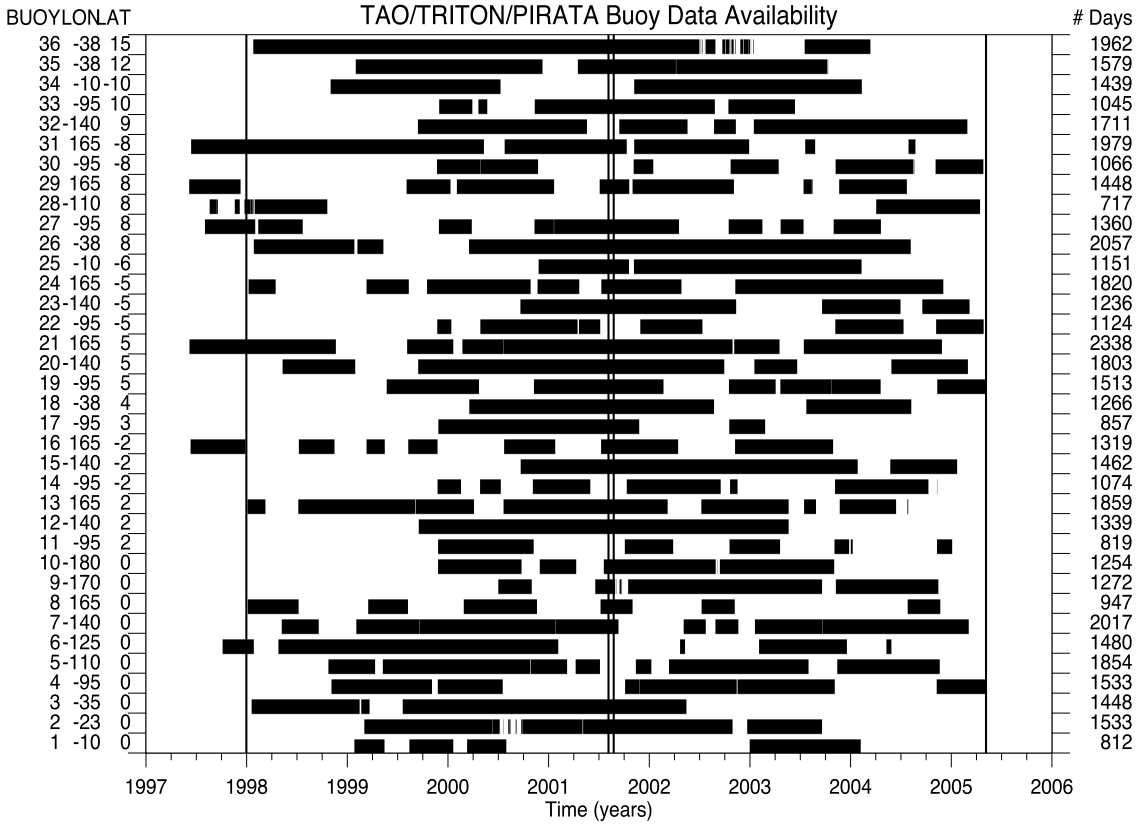

Fig. 2. Data availability for each buoy location. The single vertical lines represent the start of the pre-boost and end of the post-boost periods. The double vertical line represents the time of the orbit boost.

are raining in the PR retrievals. The gauge mean is 8.17 mm day^{-1} and the PR mean is 7.09 mm day^{-1}. The gauge means are different due to the different sample sizes. Because of the differences between the observing systems, the percent time raining is not directly comparable between the gauges and the satellite.

Figure 4 shows histograms of the matched gauge and TRMM data for buoy 21. Gauge values of less than 0.02 mm/day are considered zeroes for these histograms. Both the satellite and the gauge data are highly skewed to the right and highly leptokurtic (fat tailed). The bottom panels on Figure 4 show the differences between the satellite and buoy matches (satellite minus buoy). For both the TMI and the PR, the distributions are skewed to the right (skewness$\approx$3) and leptokurtic (kurtosis$\approx$9). The differences between the gauge and the satellite have a central mode, although both instruments show positive biases of the satellite relative to the rain gauge. Table I shows the statistics for buoy 21.

Figure 5 shows scatterplots of the TMI and PR matches with gauges at buoy 7. Buoy 7 lies outside of the ITCZ in the central Pacific in a generally dry location. At this location 2,485 matches with the TMI yield a gauge mean of 0.03 mm day^{-1} and a TMI mean of 0.18 mm day^{-1}. There are 981 PR/gauge matches, giving a gauge mean of 0.04 mm day^{-1} and a PR mean of 0.15 mm day^{-1} (Figure 5).

Figure 6 shows histograms of gauge and TRMM match data at buoy 7. Gauge values of less than 0.02 mm/day are considered zeroes for these histograms. As at the wet location, the distributions for both the gauge and TRMM data are highly skewed to the right (skewness$\approx$3) and highly leptokurtic (kurtosis$\approx$7). For this dry buoy location, both the TMI and PR have a positive bias relative to the rain gauge.Table II shows the statistics for buoy 7.

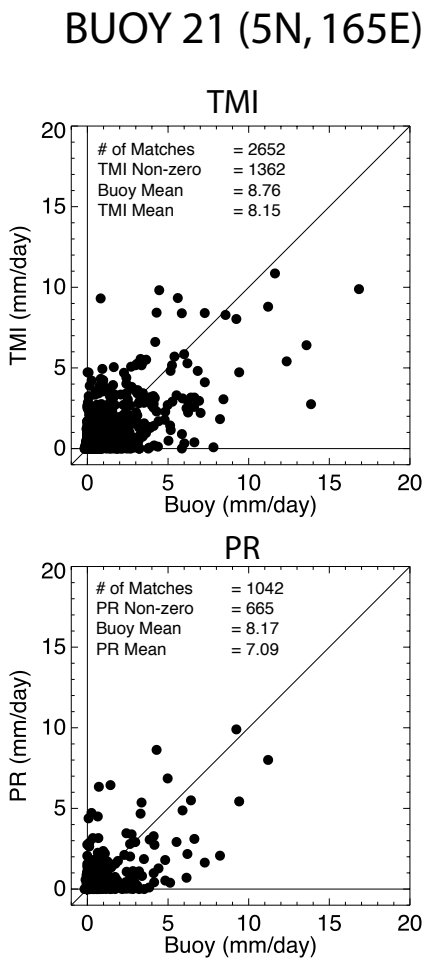

Fig. 3. Scatterplots of TMI and PR matches over the entire record at buoy 21. The time mean rainfall rates are averaged in 6-hour windows centered on TRMM overpasses.

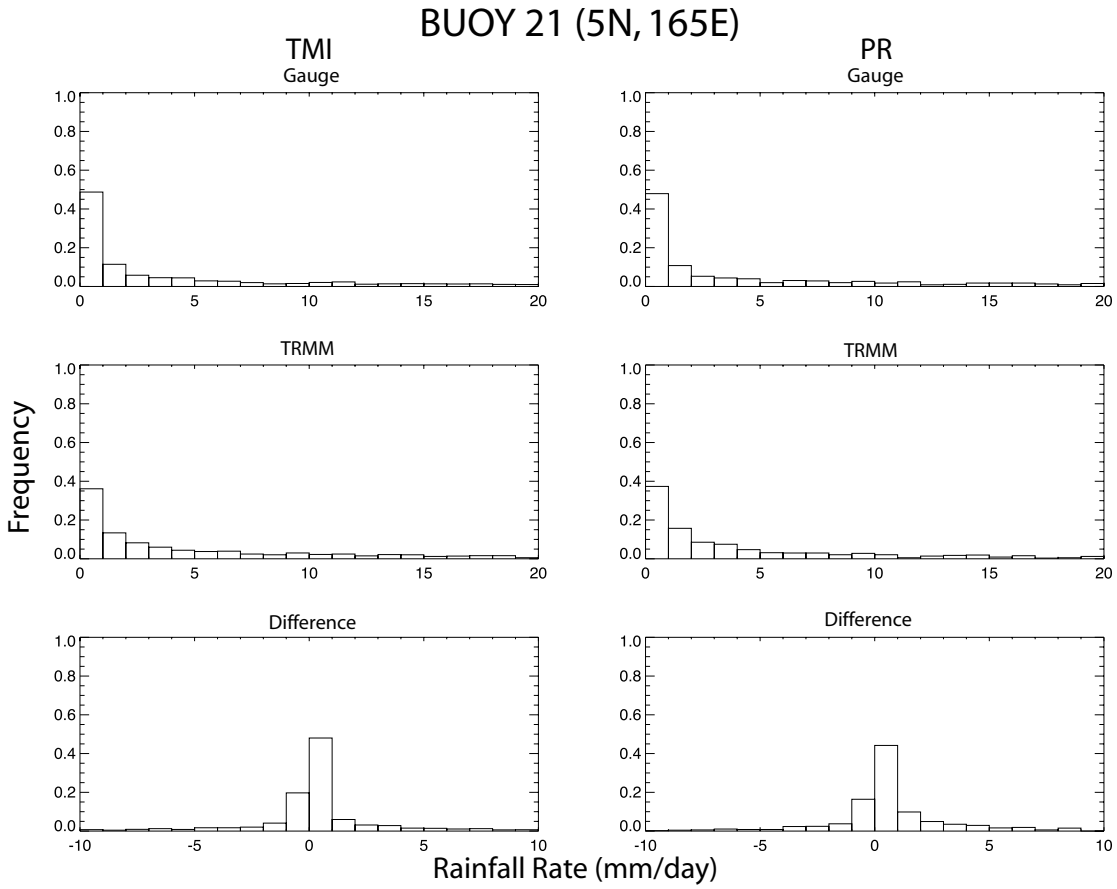

Fig. 4. Histograms of TMI and PR matches over the entire record at buoy 21. Gauge values of less than 0.02 mm day^{-1} are considered zeroes and not included. Gauge values of more than 20.0 mm day^{-1} are not included. TMI values of 0.0 mm day^{-1} and greater than 20.0 mm day^{-1} are not included. Difference values of less than -10.0 mm day^{-1} and more than 10.0 mm day^{-1} are not included.

Table I. Statistics of TRMM and buoy matched observations for Buoy 21 (5°N, 165°E). All rain rate parameters are in mm·day^{-1}.

	TMI			PR		
	Gauge	Satellite	Difference	Gauge	Satellite	Difference
Number of matches	2652	—	—	1042	—	—
% zeroes	47.4	48.6	0.7	46.7	36.2	0.8
% outside range	11.0	11.0	18.5	9.6	8.8	18.1
mean	8.8	8.2	-0.6	8.2	7.1	-1.1
variance	782.1	531.5	418.2	631.1	424.5	387.8
skewness	3.6	3.8	3.1	3.6	3.7	3.0
kurtosis	12.1	13.1	9.0	12.3	12.5	8.9
min	-4.4	0.0	-266.7	-4.3	0.0	-147.7
max	404.2	260.6	203.7	268.9	237.6	135.1

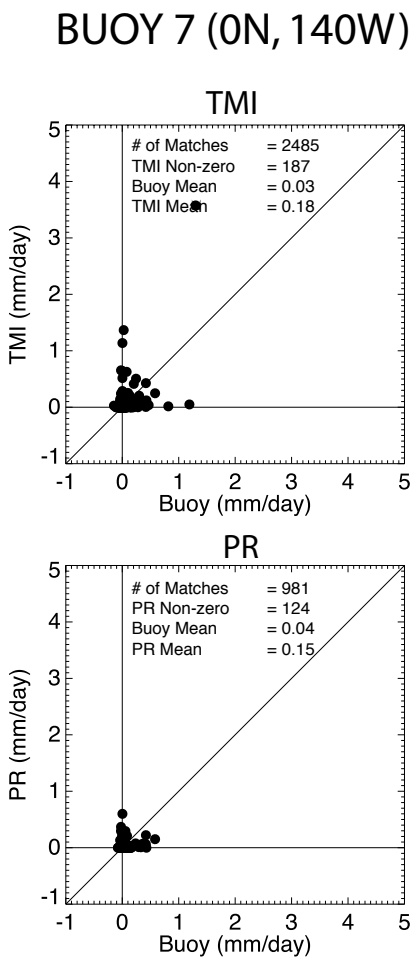

Fig. 5. Scatterplots of TMI and PR matches over the entire record at buoy 7. The time mean rainfall rates are averaged in 6-hour windows centered on TRMM overpasses.

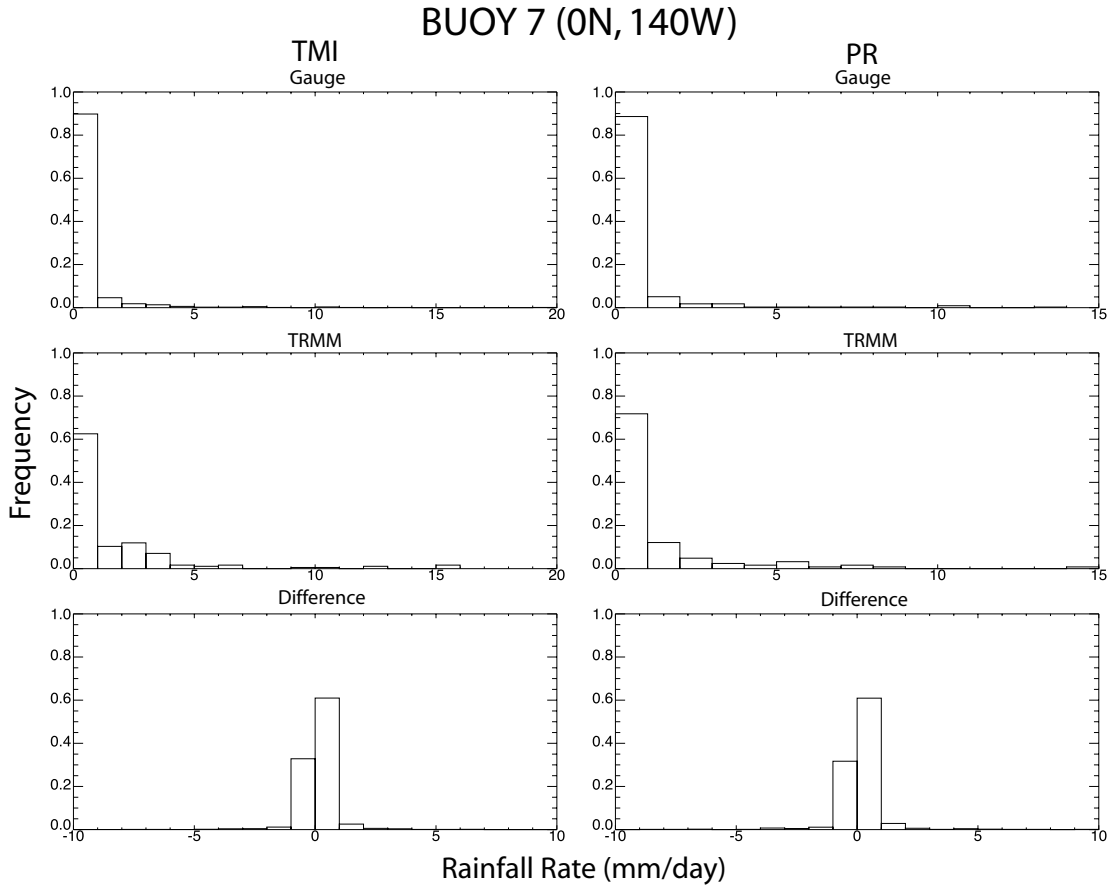

Fig. 6. Histograms of TMI and PR matches over the entire record at buoy 7. Gauge values of less than 0.02 mm day^{-1} are considered zeroes and not included. Gauge values of more than 20.0 mm day^{-1} are not included. TMI values of 0.0 mm day^{-1} and greater than 20.0 mm day^{-1} are not included. Difference values of less than -10.0 mm day^{-1} and more than 10.0 mm day^{-1} are not included.

Table II. Statistics of TRMM and buoy matched observations for Buoy 7 (0°N, 140°W). All rain rate parameters are in mm·day^{-1}.

	TMI			PR		
	Gauge	Satellite	Difference	Gauge	Satellite	Difference
Number of matches	2485	—	—	981	—	—
% zeroes	66.8	92.5	1.7	66.0	87.4	1.8
% outside range	0.1	0.1	0.4	0.0	0.0	0.3
mean	0.0	0.2	0.2	0.0	0.2	0.1
variance	1.6	4.4	3.3	1.0	0.7	1.3
skewness	3.8	3.3	2.9	3.0	3.1	2.9
kurtosis	13.2	9.4	7.2	7.4	8.4	7.4
min	-3.5	0.0	-27.4	-1.8	0.0	-10.3
max	31.2	85.9	54.6	14.0	14.4	14.3

C. Comparing time means

All of the available data matches at each gauge are used to compute time means for three time periods: the entire mission, the pre-boost period, and the post-boost period. We discuss the TMI results first.

Scatterplots of time mean values for each gauge are shown in Figure 7. The diagonal gray line is the one-to-one relationship, while the solid black line is the linear, least-squares fit to the TRMM-buoy match data. The dashed red lines represent the 95% confidence limits on the fit. The change in the slope of the linear regression reflects the change in the bias discussed in the previous paragraph. The correlation between the buoy and TMI data for all periods is high, with correlation coefficients (r^2) ≥ 0.98. The slope for the TMI over the full time period is 0.95. The slope for the linear fit of the TMI pre-boost data is 0.88, while the post-boost data have a slope of 0.99, showing very little bias relative to the gauges. The 95% confidence intervals are computed for each of the match plots, and only the TMI post-boost data are not significantly different from the one-to-one relationship.

Histograms of the time-averaged TRMM-gauge differences for the 36 buoys are shown in Figure 8. A normal distribution, computed from the sample mean and variance, is shown as the overlying curve in each plot. The TMI data are shown in the left column, and both distributions are roughly normal. It is important to note that the 36 gauges provide a relatively small sample of the tropical oceans and the differences may not be representative of the large area averages.

Table III shows the averages across all of the gauges. The TMI is biased low relative to the gauges during the pre-boost period (-0.36 mm day^{-1}), but the bias is essentially zero during the post-boost period (0.03 mm day^{-1}).

Figure 9 shows the change in bias at each gauge from pre-boost to post-boost

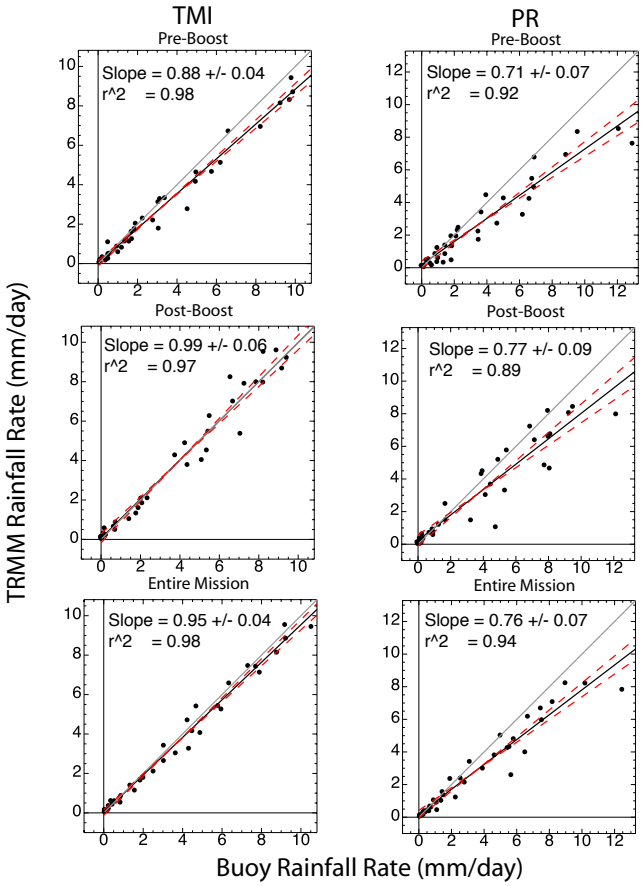

Fig. 7. Scatterplots of time-averaged TRMM and gauge rain rates. The buoy rainfall rates are on the abscissa and the TRMM rainfall rates are on the ordinate. The scale for the TMI plots (left column) is 0-10 mm day^{-1}. The scale for the PR plots (right column) is 0-12 mm day^{-1}.

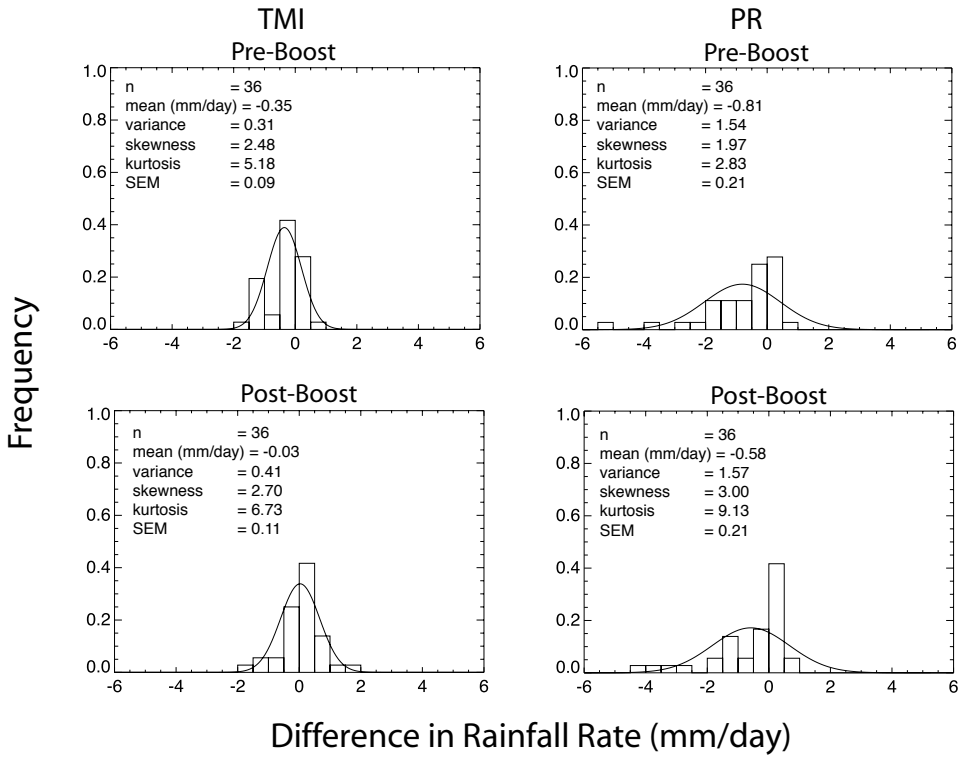

Fig. 8. Histograms of TRMM-gauge differences for all buoys. The TRMM-gauge difference in rainfall rate is on the x-axis and the frequency of measurements is on the y-axis. The left column is TMI pre- and post-boost measurements and the right column is PR pre- and post-boost measurements.

Table III. Pre-boost mean, post-boost mean, and boost change (post minus pre) are shown for TRMM, gauges, and the bias (TRMM minus gauge). Means are given in mm day^{-1} and are for all buoy/satellite matches.

	TMI			PR		
	Pre	Post	Change	Pre	Post	Change
TRMM	2.80	3.87	1.07	2.60	3.12	0.52
Gauge	3.16	3.84	0.68	3.41	3.71	0.30
Bias	-0.36	0.03	0.39	-0.81	-0.59	0.22

plotted as a function of the mean TRMM rainfall over the entire record. The left plot, showing the TMI change in bias (Equation 2.3) versus overall TMI mean rain rate, illustrates the positive change in bias seen for the TMI. Although some gauges show a negative change in bias, the majority show positive changes, with larger changes at higher rain rates. For the TMI, 29 of the 36 buoys show a positive change in bias from pre-boost to post-boost. Using the binomial distribution, the probability of at least 29 positive trials is 0.016%.

The same analysis is performed for the PR data. The PR-gauge scatterplots are shown in the right-hand panels of Figure 7. The correlations between the buoy and PR data are slightly less than for the TMI, with r^2 values from 0.89 to 0.94. This can be attributed to the smaller PR sample sizes. The slope for the PR over the full time period is 0.76. The slopes of the PR pre- and post-boost data are 0.71 and 0.78,

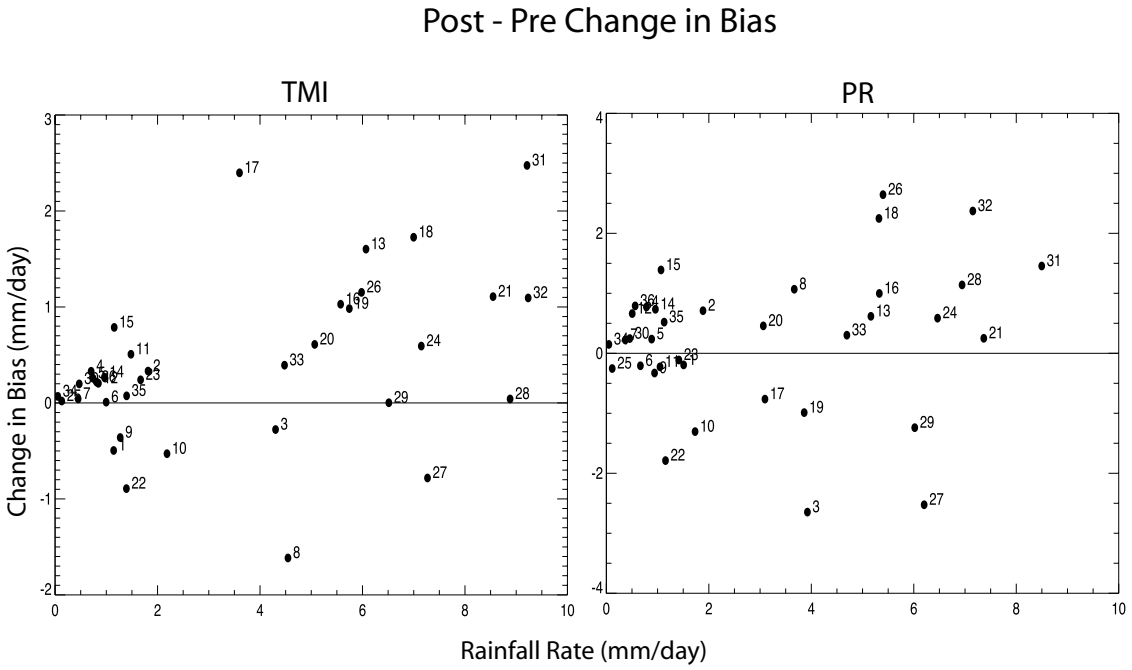

Fig. 9. Change in bias from pre-boost to post-boost (TRMM). The TRMM mean rainfall rate over the entire period is on the x-axis, and the change in TRMM bias from pre-boost to post-boost is on the y-axis.

respectively.

Histograms of the PR-gauge differences (Figure 8, right side) show that there are larger (negative) deviations of the PR from the gauge data than in the TMI data. The scatterplot of bias at each gauge versus rain rate (Figure 9) does not reveal an obvious rain rate dependence, although the statistics show a small positive change in the bias (Table III). For the PR, 23 buoys show a positive change in bias from pre-boost to post-boost. Using the binomial distribution, the probability of at least 23 positive trials is 6.62%.

The PR match means are shown on the right columns of Table III. The PR is biased low relative to the gauges during both the pre- and post-boost periods, although the magnitude of the bias is smaller for the post-boost period. The change in the bias of 0.22 mm day^{-1} is smaller than the TMI change of 0.39 mm day^{-1}.

Figure 10 shows a time series of the monthly-mean ocean rainfall rate from the TMI between 20°S and 20°N (TRMM 3A12 product). The black line represents the actual data, while the gray line is an adjustment based on the difference between pre- and post-boost mean rainfall rates. The adjusted rate is calculated by dividing the actual rainfall values by the slope of the mean values in the given boost period. The vertical line shows when the orbit boost occurred (August 7-24, 2001). The horizontal lines represent the pre- and post-boost mean rainfall rates. The mean rainfall rate of the raw TMI data over the ocean between 20°S and 20°N during the pre-boost period is 3.12 mm day^{-1}, while the post-boost mean is 3.22 mm day^{-1}.

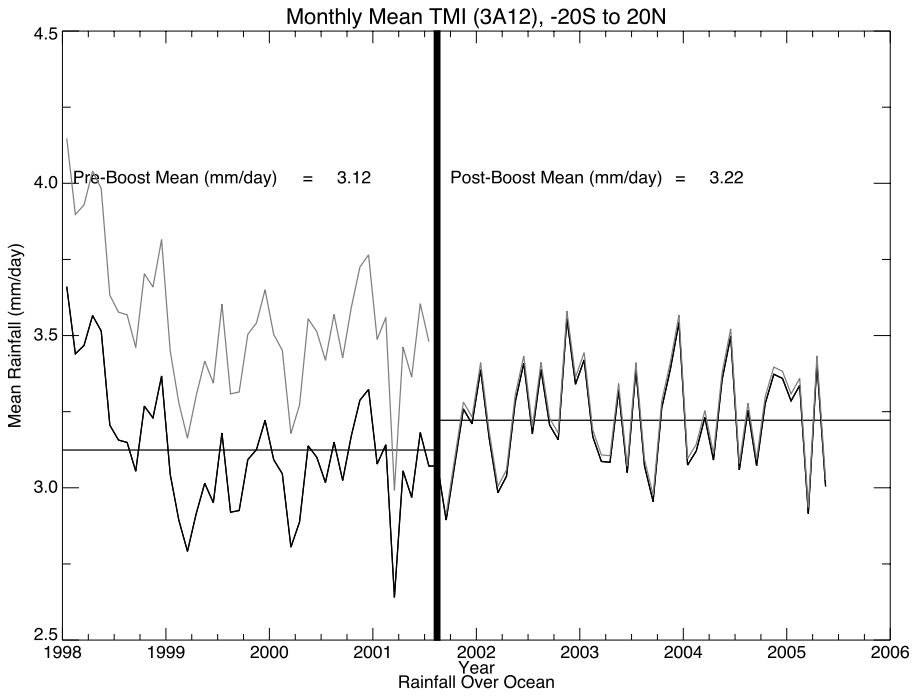

Fig. 10. Time series for raw TMI data over the ocean from 20°S to 20°N. The monthly means over the entire period are plotted. The year is on the x-axis and the TMI mean rainfall rate is on the y-axis. The vertical line represents the boost period. The horizontal lines are the pre- and post-boost means, and the gray line is the boost-adjusted mean.

CHAPTER IV

SUMMARY

The TRMM satellite orbit was boosted from ∼350 to ∼403 km in August 2001. The change in orbital altitude resulted in changes in a number of the satellite observing parameters, such as size of the fields-of-view and width of the orbit swath. In this study, rainfall retrievals from the TMI and PR instruments on the TRMM satellite are compared with surface data from rain gauges on NOAA tropical ocean buoys in order to ascertain whether the orbit boost resulted in systematic changes in the rain rate retrivals.

To improve the comparison statistics, the rain gauge data are averaged in 6-hour windows centered on the TRMM overpasses. Biases between the satellite and the gauges are evaluated by comparing the time mean differences between the satellite and the gauges, and by regressing satellite rain rates against the gauge rain rates.

When the data are stratified into pre- and post-boost periods, the TMI biases for the two periods are significantly different at the 99% level. The biases are rain rate dependent, with larger biases in regions with larger rain rates. The change in the PR bias due to the orbit boost is not statistically significant, even at the 90% level, perhaps due to the smaller sample size for the PR. Similarly, the slopes of the linear regressions are statistically different for the TMI for the pre- and post-boost periods, but not for the PR. Overall, the TMI data agree quite well with the gauges during the post-boost period, but are biased somewhat low during the pre-boost period. The PR is biased low with respect to the gauges by about 25% in both cases.

The time series in Figure 10 shows the variation of mean rainfall as measured by the TMI from month to month over the ocean. The variation within any given year is approximately 0.5 - 1.0 mm day^{-1}. As expected from the bias values, the post-boost

TMI data are much closer to the gauge-adjusted values than the pre-boost data. The effect of the orbit boost is more clearly seen in the TMI data than in the PR data, as shown by the significantly higher change in the bias of the TMI data (Figure 9).

Climatic variability and sampling error could both play a significant role in the trends and correlations observed in this study. In addition, we know that gauge measurements do not necessarily represent truth themselves, particularly with regard to wind speed effects. They are thought to be biased slightly low, which would indicate that the TMI and PR data are biased even lower (Serra and McPhaden 2003). However, the gauge measurements are currently the best available ground truth data for the tropical Atlantic and Pacific Oceans.

REFERENCES

Bowman, K., 2005: Comparison of TRMM precipitation retrievals with rain gauge data from ocean buoys. *J. Climate*, **18**, 178–190.

Bowman, K., J. Collier, G. North, Q. Wu, and E. Ha, 2005: Diurnal cycle of tropical precipitation in Tropical Rainfall Measuring Mission (TRMM) satellite and ocean buoy rain gauge data. *J. Geophys. Res.*, **110**, 1–14.

Bowman, K. P., A. Phillips, and G. North, 2003: Comparison of TRMM precipitation retrievals with rain gauge data from the TAO/TRITON buoy array. *Geophys. Res. Lett.*, **14**, 1757.

Furuzawa, F. and K. Nakamura, 2005: Differences of rainfall estimates over land by Tropical Rainfall Measuring Mission (TRMM) precipitation radar (PR) and TRMM microwave imager (TMI)–Dependence on storm height. *J. Appl. Meteorol.*, **44**, 367–383.

Hayes, S., L. Mangum, J. Picaut, A. Sumi, and K. Takeuchi, 1991: TOGA-TAO: A moored array for real-time measurements in the tropical Pacific Ocean. *Bull. Am. Meteorol. Soc.*, **72**, 339–347.

Kummerow, C., W. Barnes, T. Kozu, J. Shiue, and J. Simpson, 1998: The Tropical Rainfall Measuring Mission (TRMM) sensor package. *J. Atmos. Oceanic Technol.*, **15**, 809–817.

Kummerow, C., J. Simpson, O. Thiele, W. Barnes, A. Chang, E. Stocker, R. Adler, A. Hou, R. Kakar, F. Wentz, P. Ashcroft, T. Kozu, Y. Hong, K. Okamoto, T. Iguchi, H. Kuroiwa, E. Im, Z. Haddad, G. Huffman, B. Ferrier, W. Olson,

E. Zipser, E. Smith, T. Wilheit, G. North, T. Krishnamurti, and K. Nakamura, 2000: The status of the Tropical Rainfall Measuring Mission (TRMM) after two years in orbit. *J. Appl. Meteorol.*, **15**, 1965–1982.

Masunaga, H., T. Iguchi, R. Oki, and M. Kachi, 2002: Comparison of rainfall products derived from TRMM microwave imager and precipitation radar. *J. Appl. Meteorol.*, **41**, 849–862.

McPhaden, M., A. Busalacchi, R. Cheney, J. Donguy, K. Gage, D. Halpern, M. Ji, P. Julian, G. Meyers, G. Mitchum, P. Niiler, J. Picaut, R. Reynolds, N. Smith, and K. Takeuchi, 1998: The Tropical Ocean-Global Atmosphere (TOGA) observing system : A decade of progress. *J. Geophys. Res.*, **103**, 14,169–14,240.

Nesbitt, S., E. Zipser, and C. Kummerow, 2004: An examination of version-5 rainfall estimates from the TRMM microwave image, precipitation radar, and rain gauges on global, regional, and storm scales. *J. Appl. Meteorol.*, **43**, 1016–1036.

Serra, Y., P. A'Hearn, H. Freitag, and M. McPhaden, 2001: ATLAS self-siphoning rain gauge error estimates. *J. Atmos. Oceanic Technol.*, **18**, 1989–2002.

Serra, Y. and M. McPhaden, 2003: Multiple time- and space-scale comparisons of ATLAS buoy rain gauge measurements with TRMM satellite precipitation measurements. *J. Appl. Meteor.*, **42**, 1,045–1,059.

VITA

Jeremy DeMoss received a B.S. degree in biology from Union University, Jackson, TN in 2004. He then was admitted to the Department of Atmospheric Sciences at Texas A&M University in August 2004 to pursue a master's degree. He can be reached at the Department of Atmospheric Sciences, Texas A&M University, College Station, 77843-3150. Email: jeremydemoss@tamu.edu.

The typist for this thesis was Jeremy DeMoss.